Available online at www.sciencedirect.com

ScienceDirect

Ceramics International 35 (2009) 3469–3474

CERAMICS INTERNATIONAL

www.elsevier.com/locate/ceramint

Electrophoretically deposited manganese oxide coatings for supercapacitor application

Chin-Yi Chen [a], Sheng-Chang Wang [b], Chia-Yen Lin [a],
Fan-Shiong Chen [c], Chung-Kwei Lin [a,*]

[a] *Department of Materials Science and Engineering, Feng Chia University, No. 100, Wenhwa Rd., Seatwen, Taichung 407, Taiwan*
[b] *Department of Mechanical Engineering, Southern Taiwan University, No. 1 Nantai St., Yungkang City, Tainan 710, Taiwan*
[c] *Department of Materials Engineering, Tatung University, No. 40, Sec. 3, Jhongshan N. Rd., Taipei 104, Taiwan*

Received 17 November 2008; received in revised form 30 April 2009; accepted 26 June 2009
Available online 16 July 2009

Abstract

In the present study, manganese oxide electrodes with promising pseudo-capacitive properties were prepared by electrophoretic deposition (EPD) using needle-like manganese dioxide powders. As-deposited coating exhibited a porous microstructure where the size and shape of the starting powders can be observed. The electrochemical performance of the as-deposited coating was then evaluated by cyclic voltammetry (CV) up to 300 times. The initial specific capacitance was 236 F/g which dropped to 200 F/g after 25 CV tests, and decreased gradually to 190 F/g thereafter. The electrochemical behaviors during EPD and CV were examined by synchrotron X-ray absorption spectroscopy techniques from which it was deciphered that a reduction reaction from Mn^{4+} to Mn^{3+} occurred during EPD concomitant with re-oxidization during repetitive CV cycles.

Keywords: A. Films; B. Spectroscopy; B. X-ray method; E. Capacitors

---

1. Introduction

Electrochemical supercapacitors have attracted increasing research interests due to their unique characteristics in terms of power and energy density and can be used for applications requiring a high power output and/or a high cycle capacity [1,2]. The conventional oxides used as the electrodes of supercapacitors are relatively expensive materials, such as RuO_2 or IrO_2 [3,4]. Relatively cheap and easily available transition metal oxides that possess multi-valence characteristics can prove to be potential alternatives to these conventional oxides. For instance, manganese oxides with its multiple manganese valence states are promising supercapacitor materials due to the low cost of raw materials and the fact that manganese is considered more environmental friendly than other noble metal oxides [5–7].

Considerable efforts have been made in this direction for the preparation of manganese oxide films and coatings using various well-known techniques such as physical vapor deposition [8], chemical vapor deposition [9], anodic deposition [10,11], cathodic deposition [12], and sol–gel process [13,14], etc. [15]. These processes deposit manganese and/or its oxide molecules or islands onto substrates to form dense manganese oxide electrodes. Electrophoretic deposition (EPD) on the other hand is a relatively simple process, involving motion of charged particles in an aqueous medium followed by deposition onto substrates under an applied electric field. This technique has been effectively used to deposit coatings for various applications [16]. For instances, functionally graded materials [17], patterned electrodes [18], sensors and functional ceramics [19], and fuel cells [20] have been successfully prepared by EPD.

Manganese oxides exhibit catalytic properties may experience gas evolution during EPD process where an applied field is inevitable. Gas evolution due to reduction of manganese oxide or dissociation of water may make the EPD of manganese oxide difficult. Though we have demonstrated that spray-pyrolyzed powders can be electrophoretically deposited to obtain porous electrodes, however, only limited gas evolution during EPD was noticed [21,22]. In the present

---

* Corresponding author. Tel.: +886 4 24517250x5309; fax: +886 4 24510014.
E-mail address: cklin@fcu.edu.tw (C.-K. Lin).

0272-8842/$36.00
doi:10.1016/j.ceramint.2009.06.025

study, commercial available needle-like manganese dioxide powders with high surface area and catalytic properties will be electrophoretically deposited onto graphite substrates to obtain porous manganese oxide electrodes. Corresponding structural changes and electrochemical properties of the as-deposited coatings during the preparation and characterizations will be investigated.

2. Experimental procedures

Manganese dioxide powders (major phase: α-phase MnO_2 >98.0 wt.%, minor phases: other Mn oxides, Songsing Nano Technology Co., Ltd., Taiwan) prepared by the wet-chemical process were used as the precursor for electrophoretical deposition on graphite substrates. The substrates with a dimension of 10 mm × 10 mm × 3 mm were ground, degreased, etched in 0.2 M H_2SO_4, and rinsed by deionized water. The pretreated graphite substrates were then insulated by PTFE films and thus only an area of 1 cm × 1 cm was exposed for deposition. The manganese oxide powders were dispersed into an ethanol base solution (99.5 wt.%, Echo Chemical Co., Ltd., Taiwan) and ultrasonically mixed for 30 min with 1 ml of 10 wt.% H_2SO_4 (Shimakyu's Pure Chemicals, Japan). The suspension for EPD was prepared to a solid load concentration of 0.2 g/l. EPD was performed under a potentiostatic mode by a DC power supply at 100 V for 20 min leading to cathodic deposits on the graphite substrates. The electrode was weighed before and after the EPD deposition process by a microbalance with an accuracy of 10 μg (Sartorius 235S, Germany). The mass of the powder coating was controlled at ~0.1 mg on each substrate for achieving optimum electrochemical performance of the coating.

Phase identification of powders and as-deposited coatings was performed using X-ray diffractometry (XRD, MAC-MXP3, Japan) with a Cu K_α radiation. The starting powder was also examined by transmission electron microscopy (TEM, JEM-2010, JEOL, Japan). The surface morphology of the EPD films before and after cyclic voltammetry (CV) was observed by a field-emission scanning electron microscopy (FE-SEM, HITACHI S4800, Japan). In addition synchrotron X-ray absorption spectroscopy (XAS) technique was used to decipher the electronic properties and localized variations in atomic environment. The XAS experiments were performed at the HSGM (20A, 100–1500 eV) and Wiggler-C (17C, 4–15 keV) beamlines at the National Synchrotron Radiation Research Center (NSRRC) in Hsinchu, Taiwan.

Cyclic voltammetry (CV) performances were evaluated by an electrochemical analyzer (CH Instruments, Model 600B, USA) using a standard three-electrode cell system in 1 M Na_2SO_4 solution at room temperature. The as-deposited manganese oxide film was used as the working electrode, while a gold disk and an Ag/AgCl electrode were used as the counter and reference electrode, respectively. The CV scan rate was set at 25, 50, or 100 mV/s within a potential ranged from 0 to 1 V. The area under the CV curve was used to estimate the specific capacitance of the powder coating on the substrate.

3. Results and discussion

The stability of the crystallinity of MnO_x supercapacitors is imperative for enhancement of performance efficiency. For instances, phase stability during an acid or basic environment, and/or elevated temperature may degrade the coating quality. Hence, X-ray diffraction of the as-received manganese oxide as a function of temperature (Fig. 1) was investigated for validating the inception of new phases with temperature besides confirming the crystalline stability. As seen from the figure (Fig. 1), it should be pointed out that no significant differences can be revealed for manganese oxide heating at a temperature lower than 500 °C. All of the manganese oxide exhibited an α-MnO_2 phase. In addition, peak broadening implying an extremely small grain size (~10 nm calculated from the Scherrer's formula) of the α-MnO_2, even after heating at 500 °C, was observed. Partial α-MnO_2 transformation into Mn_2O_3 can be observed when the heating temperature was 600 °C. This shows a similar trend as reported in the literature [23] and indicates that the α-MnO_2 used in the present study is stable up to a temperature of 500 °C.

In addition to the thermal stability examination, the peak broadening in XRD pattern as shown in Fig. 1 may indicate that the starting materials, even those heat-treated at a temperature lower than 500 °C, were nanocrystalline. Fig. 2 shows the transmission electron microscope image of the starting α-MnO_2 phase powders that exhibited an obvious needle-like microstructure with a diameter of ~10 nm and a length ranged from 50 to 400 nm, showing good agreement with the XRD data. Because the electrochemical reaction between electrode materials and electrolyte solution is generally thought to take place on the surface of the electrode, the larger is the surface area of the electrode, the higher specific capacitance can be obtained. It has been reported that these nanocrystalline needle-like manganese dioxide exhibited a relatively high surface energy and possessed significant potential in practical use of supercapacitor [24]. In the present study, the nanocrystalline needle-like manganese dioxide powders were then electrophoretically deposited onto a graphite substrate and the electrochemical performances of these electrodes were investigated.

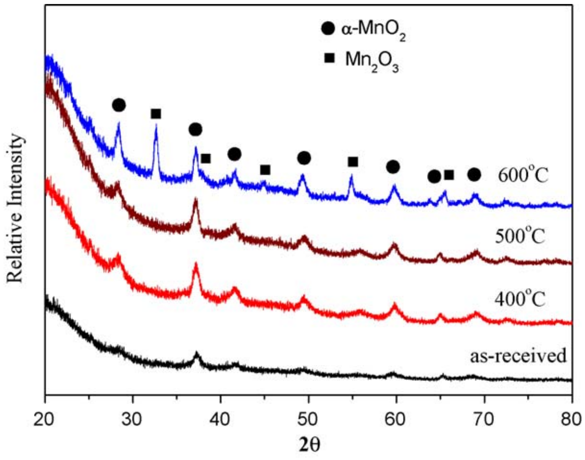

Fig. 1. XRD patterns of manganese oxide films heating at various temperatures.

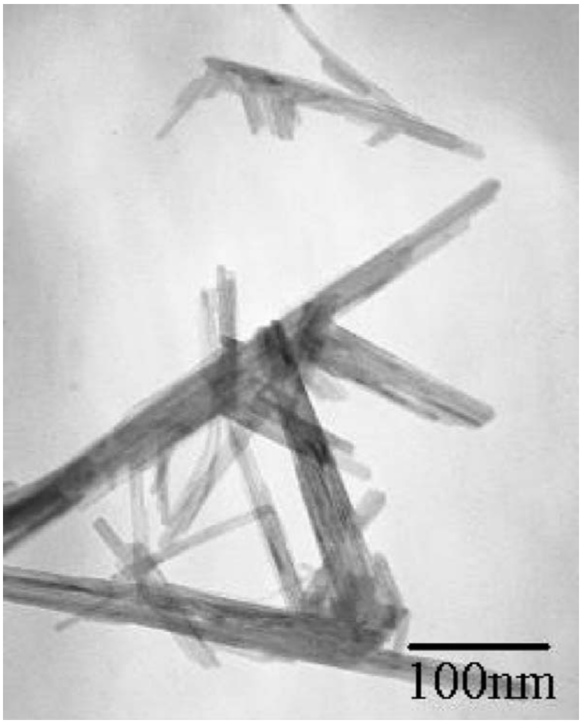

Fig. 2. TEM micrograph of as-obtained needle-like manganese oxide powder.

Fig. 3 shows the scanning electron microscope image of the manganese oxide films prepared by electrophoretic deposition (EPD) process. It can be noted from Fig. 3 that the as-deposited films still exhibited the needle-like microstructure. Bundles of manganese oxide needle-like powders can be observed from the SEM image. This indicates that agglomeration of starting powders occurred during the EPD process. It should also be pointed out that gas bubble evolution can be noticed during the EPD process. This may be attributed to the reduction reaction of MnO_2 or dissociation of water and acts as an impediment for the EPD of manganese oxide films. Thus, limited research concerning preparation of manganese oxide films by EPD has been reported [21,22]. The relevant cathodic reaction of the positively charged particles during EPD can most likely be represented by an equation of the type:

$$2MnO_2(H_3O^+) + 2e^- \rightarrow Mn_2O_3 + 3H_2O$$

where the product of Mn_2O_3 phase is identified by the XAS analysis. The corresponding gas evolution reaction resulting from the dissociation of water is given by:

$$H_2O + e^- \rightarrow \tfrac{1}{2}H_{2(g)} + OH^-$$

Therefore, it is suspected that the evolved hydrogen may cause a portion of the reduction of the deposited MnO_2 powder on the cathode. In addition to the phase transition and gas evolution, a porous microstructure was also achieved. It has been reported that a porous microstructure was beneficial to the electrolyte passage and may be contributed to improve the electrochemical properties [24,25]. For instance, porous manganese oxide films prepared by sol–gel process exhibited a better performance than the relatively smooth one [13]. The supercapacitive properties of the as-prepared manganese oxide films were evaluated by cyclic voltammetry.

Fig. 4 shows the specific capacitance as a function of CV cycle number for the manganese oxide electrode prepared by an electrophoretic deposition starting from needle-like manganese oxide powders. It is interesting to note that the specific capacitance for the first cycle exhibited the maximum value of 236 F/g. An abrupt decrease from the maximum (236 F/g) to 215 and 200 F/g after 15 and 25 cycles of CV tests, respectively. The specific capacitance approximately exhibited a linear relationship with a negative slope for the first 25 CV tests and only showed slight decrease thereafter. It is suspected that the loose bundle-like manganese oxide powders only exhibited weak bonding (such as van der Waals force) without strong chemical bonding and, thus, induced a significant decrease during the first few cycles (25 cycles in the present study) of CV tests. The repetitive charging and discharging CV cycles increased gradually the bonding strength among the bundles of needle-like powders. A relatively stable structure of manganese oxide electrode was gradually achieved and the specific capacitance only decreased slightly from 200 F/g (25th cycle) to 190 F/g (300th cycle). In summary, the specific capacitance

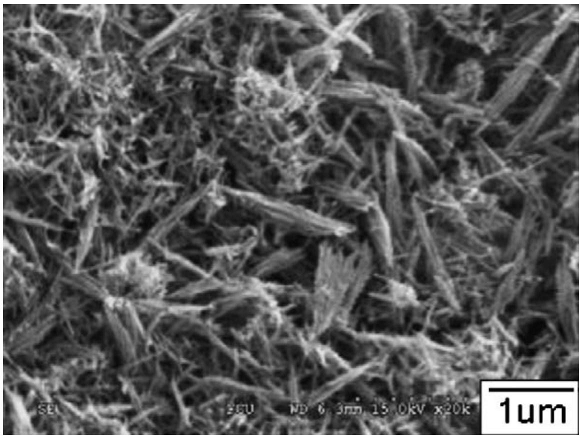

Fig. 3. SEM micrographs of as-deposited manganese oxide coatings.

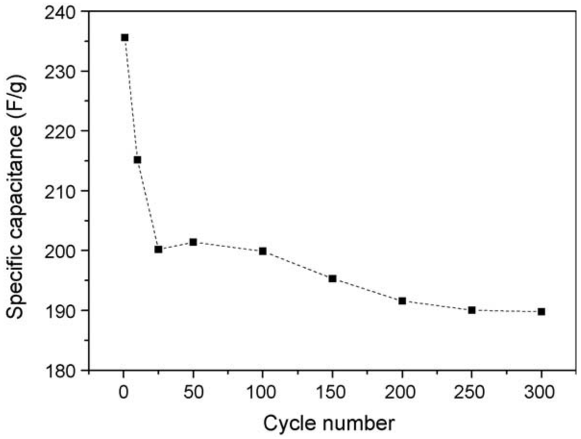

Fig. 4. Variation of specific capacitance with respect to CV cycle number for manganese oxide coating.

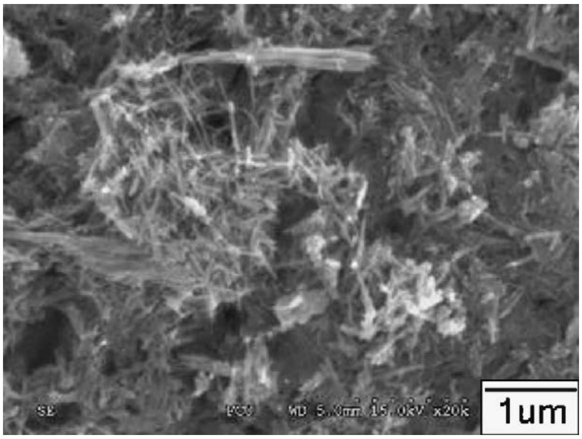

Fig. 5. SEM micrographs of manganese oxide coatings after CV tests.

exhibited a significant decrease of 15.3% (from 236 to 200 F/g) for the first 25 cycles and only a slight decrease of 5.0% (200–190 F/g) for the next 275 cycles.

Fig. 5 shows the SEM image of the manganese oxide films after 300 CV tests. As compared to that shown in Fig. 3 (the manganese oxide film as-prepared by EPD process), it can be noted that, after 300 CV tests, not only the relative amount of bundles of needle-like powders significantly decreased, but also the relatively porous structure gradually destructed. This can be attributed to the charging-and-discharging CV cycles induced repetitive decomposition-and-precipitation processes [22,26]. Although the porous structure gradually deteriorated due to exposure to CV cyclic tests, the pores, retained their effectiveness for passage of electrolyte even after 300 CV tests. Thus, only a slight decrease in specific capacity was observed after the first 25 cycles.

In addition to the electrochemical performance evaluated by repetitive CV tests as discussed above in Fig. 3, the electrochemical behavior of the manganese oxide electrode was investigated by CV examined at various scan rates. Fig. 6 shows the CV curves tested at scan rates of 25, 50, and 100 mV s^{-1} and the corresponding specific capacitance was 215.2, 211.8, and 205.9 F/g, respectively. The measured CV values were compatible to those reported in the literatures [7,27]. It can be noted that the CV curve tested at a scan rate of 25 mV s^{-1} was close to a rectangular shape, exhibited mirror-image characteristics, and revealed good reversibility and relatively ideal pseudo-capacitive behavior. The rectangular shape distorted gradually with increasing scan rate. This indicates that the pseudo-capacitive behavior deviates from its ideality with increasing scan rate. Meanwhile, higher the scan rate the smaller the measured specific capacitance. This shows a similar trend reported in the literature [28,29] and can be attributed to the less effective interaction between the ions and the electrode at higher scan rates [29].

In order to reveal further the structural variations within three different stages of these needle-like MnO_2 (starting powders and coatings before and after CV test), synchrotron X-ray absorption spectroscopy (XAS) technique was used. An XAS spectrum, basically the measured X-ray absorption coefficient as a function of the incoming photon energy, includes X-ray absorption near-edge structure (i.e., XANES) and extended X-ray absorption fine structure (i.e., EXAFS). For a specific examined element, XANES elucidates the electronic structure, while EXAFS investigates the local atomic structure concerning the type and number of element, and nearest neighbor bond length [30–32]. Fig. 7 shows the EXAFS spectra at Mn K edge of the starting powders and coatings before and after CV test. It can be noted that the XANES spectrum of as-deposited coating (i.e., coating before CV test) differed from the other two spectra. A decrease in the Mn K absorption edge of ~2 eV within the as-deposited coating can be noticed. This indicates that manganese valence decreased from +4 of MnO_2 to ~+3 of Mn_2O_3 during the EPD process [22]. The decrease in manganese valence, however, was recovered during the repetitive decomposition-and-precipitation processes of CV tests.

The differences in local atomic environment can be revealed better after Fourier transformation of the EXAFS spectra [33] and, thus, the radial distribution function (RDF) of the local atomic environment of detected element (i.e., Mn) can be observed. Fig. 8 shows the RDFs corresponding to those in

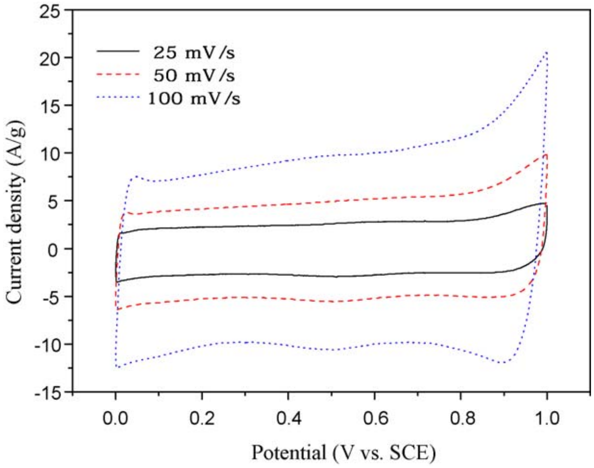

Fig. 6. CV curves tested at different scan rates for the manganese oxide coatings.

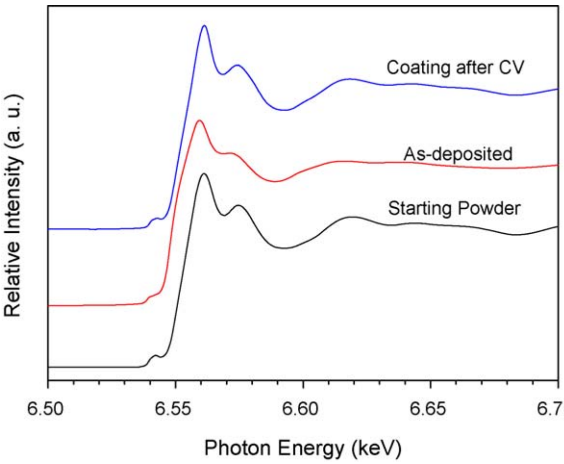

Fig. 7. EXAFS spectra at Mn K edge for manganese oxide powder and coatings before and after CV tests.

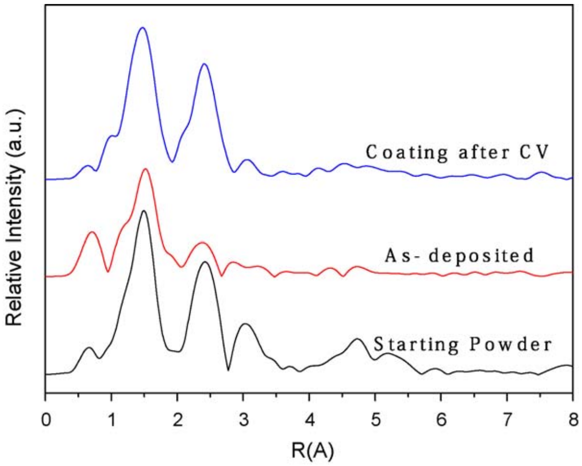

Fig. 8. Radial distribution functions for manganese oxide powder and coatings before and after CV tests.

Fig. 7. It can be noticed that, compared the RDFs of starting powder and the as-deposited coating, the EPD process did induce a structural variation. In addition, though the decrease in manganese valence can be recovered by repetitive CV tests, slight differences in high order peaks (the peak at 3 Å, and the other at larger distances) can be noticed. This indicates a coating degradation that may be responsible for the decrease in specific capacitance.

Synchrotron X-ray absorption spectroscopy shown in Figs. 7 and 8 examined a certain amount of the coatings due to relatively high photon energy around Mn K edge (6539 eV), surface-sensitive examinations were performed at Mn L edge and Fig. 9 shows the corresponding XANES spectra. The starting powder and coating after CV exhibited a relatively stronger peak at 643.1 eV (corresponding to Mn^{4+}). The 643.1 eV peak intensity decreased and accompanied by an increase in 641.5 eV and 640.0 V peaks coinciding with Mn_2O_3 and Mn_3O_4, respectively [34,35]. This suggested that Mn^{4+} reduced to Mn^{3+} (or $Mn^{2.67+}$) during the EPD process and gradually oxidized back to Mn^{4+} during repetitive CV tests.

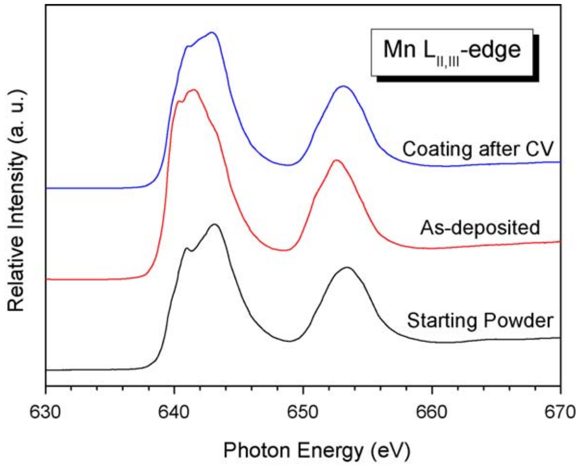

Fig. 9. EXAFS spectra at Mn L edge for manganese oxide powder and coatings before and after CV tests.

4. Conclusions

Needle-like manganese dioxide powders with a diameter of ~10 nm and a length ranging from 50 to 400 nm were electrophoretically deposited onto graphite substrates. As-deposited coating exhibited a porous microstructure where the size and shape of starting powders can be observed. Relative weak bonding was responsible for the initial electrochemical instability where the specific capacitance decreased ~15% from 236 F/g (1st cycle) to 200 F/g (25th cycle). Only slight decrease (5%, from 200 to 190 F/g) was noticed for the next 275 cycles. Synchrotron X-ray absorption spectroscopy examination revealed that manganese oxide electrodes experienced mainly a reduction reaction from Mn^{4+} to Mn^{3+} during EPD process and gradually recovered to tetravalent manganese during repetitive CV tests.

Acknowledgements

The authors would like to thank the National Science Council of Taiwan for financially supporting this work under Grant No. NSC 94-2216-E-035-008. The authors also thank the entire staff at NSRRC (Hsinchu, Taiwan, ROC) for the expertise assistance.

References

[1] B.E. Conway, Electrochemical Supercapacitors, Kluwer-Plenum, New York, 1999.
[2] B.E. Conway, Transition from supercapacitor to battery behavior in electrochemical capacitor, Journal of Electrochemical Society 138 (6) (1991) 1539–1548.
[3] J.P. Zheng, T.R. Jow, A new charge storage mechanism for electrochemical capacitors, Journal of Electrochemical Society 142 (1) (1995) L6–L8.
[4] J.P. Zheng, P.J. Cygan, T.R. Jow, Hydrous ruthenium oxide as an electrode material for electrochemical capacitors, Journal of Electrochemical Society 142 (8) (1995) 2699–2703.
[5] J.N. Broughton, M.J. Brett, Investigation of thin sputtered Mn films for electrochemical capacitors, Electrochimica Acta 49 (25) (2004) 4439–4446.
[6] B. Djurfors, J.N. Broughton, M.J. Brett, D.G. Ivey, Electrochemical oxidation of Mn/MnO films: formation of an electrochemical capacitor, Acta Materialia 53 (4) (2005) 957–965.
[7] Y.S. Chen, C.C. Hu, Capacitive characteristics of binary manganese–nickel oxides prepared by anodic deposition, Electrochemical and Solid-State Letters 6 (10) (2003) A210–A213.
[8] B. Djurfors, J.N. Broughton, M.J. Brett, D.G. Ivey, Microstructural characterization of porous manganese thin films for electrochemical supercapacitor applications, Journal of Materials Science 38 (24) (2003) 4817–4830.
[9] T. Maruyama, Y. Osaki, Electrochromic properties of manganese oxide thin films prepared by chemical vapor deposition, Journal of Electrochemical Society 142 (9) (1995) 3137–3141.
[10] C.C. Hu, T.W. Tsou, Capacitive and textural characteristics of hydrous manganese oxide prepared by anodic deposition, Electrochimica Acta 47 (21) (2002) 3523–3532.
[11] J.K. Chang, W.T. Tsai, Microstructure and pseudocapacitive performance of anodically deposited manganese oxide with various heat-treatments, Journal of Electrochemical Society 152 (10) (2005) A2063–A2068.
[12] N. Nagarajan, H. Humadi, I. Zhitomirsky, Cathodic electrodeposition of MnOx films for electrochemical supercapacitors, Electrochimica Acta 51 (15) (2006) 3039–3045.

[13] S.C. Pang, M.A. Anderson, T.W. Chapman, Novel electrode materials for thin-film ultracapacitors: comparison of electrochemical properties of sol–gel-derived and electrodeposited manganese dioxide, Journal of Electrochemical Society 147 (2) (2000) 444–450.

[14] S.F. Chin, S.C. Pang, M.A. Anderson, Material and electrochemical characterization of tetrapropylammonium manganese oxide thin films as novel electrode materials for electrochemical capacitors, Journal of Electrochemical Society 149 (4) (2002) A379–A384.

[15] A. Bai, C.C. Hu, Effects of electroplating variables on the composition and morphology of nickel–cobalt deposits plated through means of cyclic voltammetry, Electrochimica Acta 47 (21) (2002) 3447–3456.

[16] P. Sarkar, P.S. Nicholson, Electrophoretic deposition (EPD): mechanisms, kinetics, and application to ceramics, Journal of the American Ceramic Society 79 (8) (1996) 1987–2002.

[17] S. Put, J. Vleugels, G. Anne, O. Van der Biest, Functionally graded ceramic and ceramic–metal composites shaped by electrophoretic deposition, Colloids and Surfaces A 222 (1–3) (2003) 223–232.

[18] N. Ogata, J. Van Tassel, C.A. Randall, Electrode formation by electrophoretic deposition of nanopowders, Materials Letters 49 (1) (2001) 7–14.

[19] N. Dougami, T. Takada, Modification of metal oxide semiconductor gas sensor by electrophoretic deposition, Sensors and Actuators B 93 (1–3) (2003) 316–320.

[20] I. Zhitomirsky, A. Petric, Electrophoretic deposition of ceramic materials for fuel cell applications, Journal of the European Ceramic Society 20 (12) (2000) 2055–2061.

[21] C.Y. Chen, C.K. Lin, Y.R. Lyu, H.H. Lin, W.H. Tuan, Pseudocapacitive manganese oxide prepared by a spray pyrolysis/electrostatic deposition technique, Advances in Science and Technology 45 (2006) 1896–1901.

[22] C.Y. Chen, Y.R. Lyu, C.Y. Su, H.M. Lin, C.K. Lin, Characterization of spray pyrolyzed manganese oxide powders deposited by electrophoretic deposition technique, Surface and Coatings Technology 202 (4–7) (2007) 1277–1281.

[23] M. Toupin, T. Brousse, D. Belanger, Influence of microstructure on the charge storage properties of chemically synthesized manganese dioxide, Chemistry of Materials 14 (9) (2002) 3946–3952.

[24] M. Wu, G.A. Snook, G.Z. Chen, D.J. Fray, Redox deposition of manganese oxide on graphite for supercapacitors, Electrochemistry Communications 6 (5) (2004) 499–504.

[25] G.-X. Wang, B.-L. Zhang, Z.-L. Yu, M.-Z. Qu, Manganese oxide/MWNTs composite electrodes for supercapacitors, Solid State Ionics 176 (11–12) (2005) 1169–1174.

[26] S.-C. Wang, C.-Y. Chen, T.-C. Chien, P.-Y. Lee, C.-K. Lin, Supercapacitive properties of spray pyrolyzed iron-added manganese oxide powders deposited by electrophoretic deposition technique, Thin Solid Films 517 (3) (2008) 215–218.

[27] H. Kim, B.N. Popov, Synthesis and characterization of MnO_2-based mixed oxides as supercapacitors, Journal of Electrochemical Society 150 (3) (2003) D56–D62.

[28] J.K. Chang, W.T. Tsai, Material characterization and electrochemical performance of hydrous manganese oxide electrodes for use in electrochemical pseudocapacitors, Journal of Electrochemical Society 150 (10) (2003) A1333–A1338.

[29] V. Subramanian, H. Zhu, R. Vajtai, P.M. Ajayan, B. Wei, Hydrothermal synthesis and pseudocapacitance properties of MnO_2 nanostructures, The Journal of Physical Chemistry B 109 (43) (2005) 20207–20214.

[30] E.A. Stern, Theory of the extended X-ray-absorption fine structure, Physical Review B 10 (8) (1974) 3027–3037.

[31] F.W. Lytle, D.E. Sayers, E.A. Stern, Extended X-ray-absorption fine-structure technique. II. Experimental practice and selected results, Physical Review B 11 (12) (1975) 4825–4835.

[32] E.A. Stern, D.E. Sayers, F.W. Lytle, Extended X-ray-absorption fine-structure technique. III. Determination of physical parameters, Physical Review B 11 (12) (1975) 4836–14836.

[33] C.K. Lin, P.Y. Lee, J.L. Yang, C.Y. Tung, N.F. Cheng, Y. Hwu, EXAFS studies of amorphous $Fe_{50}Ta_{50}$ powders during mechanical alloying, Journal of Non-Crystalline Solids 232–234 (1998) 520–525.

[34] C. Colmenares, S. Deutsch, C. Evans, A.J. Nelson, L.J. Terminello, J.G. Reynolds, J.W. Roos, I.L. Smith, Analysis of manganese particulates from automotive decomposition of methylcyclopentadienyl manganese tricarbonyl, Applied Surface Science 151 (3–4) (1999) 189–202.

[35] H. Kurata, C. Colliex, Electron-energy-loss core–edge structures in manganese oxides, Physical Review B 48 (4) (1993) 2102–2108.